

NJC

Accepted Manuscript



This is an *Accepted Manuscript*, which has been through the Royal Society of Chemistry peer review process and has been accepted for publication.

Accepted Manuscripts are published online shortly after acceptance, before technical editing, formatting and proof reading. Using this free service, authors can make their results available to the community, in citable form, before we publish the edited article. We will replace this *Accepted Manuscript* with the edited and formatted *Advance Article* as soon as it is available.

You can find more information about *Accepted Manuscripts* in the [Information for Authors](#).

Please note that technical editing may introduce minor changes to the text and/or graphics, which may alter content. The journal's standard [Terms & Conditions](#) and the [Ethical guidelines](#) still apply. In no event shall the Royal Society of Chemistry be held responsible for any errors or omissions in this *Accepted Manuscript* or any consequences arising from the use of any information it contains.

Cite this: DOI: 10.1039/c0xx00000x

www.rsc.org/xxxxxx

ARTICLE TYPE

Novel Fluorescence Resonance Energy Transfer Optical Sensors for Vitamin B12 Detection using Thermal Reduced Carbon Dots

Jilong Wang,^a Junhua Wei,^a Siheng Su,^a and Jenny Qiu^{*a}

Received (in XXX, XXX) Xth XXXXXXXXX 20XX, Accepted Xth XXXXXXXXX 20XX

DOI: 10.1039/b000000x

Abstract

In this paper, a novel thermal-reduced carbon dots (t-CDs) based fluorescence resonance energy transfer (FRET) sensor for determination of vitamin B₁₂ (VB₁₂) in aqueous solution is reported. Carbon dots (CDs) have attracted great attention due to their excellent tunable optical properties, low cost, easy fabrication and low toxicity, which makes them an ideal candidate for optical sensors. Through esterification reactions, blue luminescent t-CDs were prepared from carbonization of citric acid and thermally reduced by thermo gravimetric analyzer. After thermal reduction, the quantum yield of t-CDs demonstrated a 5-fold increment, which makes t-CDs an excellent donor in FRET process. The t-CDs were used to detect VB₁₂ with the concentration ranging from 1 to 12 μg/ml and their limit of detection (LOD) was as low as 0.1 μg/ml. The as-synthesized t-CDs based optical probing technique demonstrates to be simple, cost-effective, sensitive and selective for detecting biologically significant VB₁₂.

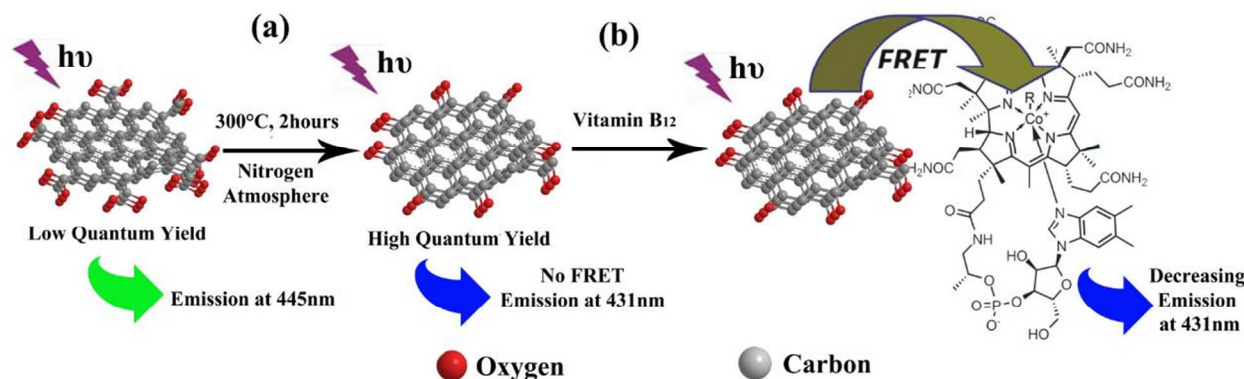
1. Introduction

Vitamins are known essential organic compounds needed for functioning healthy humans. Vitamin B₁₂ (VB₁₂) is one of a series of cobalt tetraazamacrocyclic complexes, which plays a vital role in red blood cell formation and nerve cell maintenance.¹⁻³ VB₁₂ deficiency causes severe and irreversible damage, such as anemia, metabolic abnormalities and psychosis. Extravagant absorption of VB₁₂ may also leads to unexpected adverse effects. Therefore, determination of VB₁₂ has received tremendous attention in the last decades. Traditional approaches like high-performance liquid chromatography (HPLC), chemiluminescence and atomic absorption spectrometry are widely applied to detect VB₁₂ with high sensitivity.⁴⁻⁸ Unfortunately, the above-mentioned detection techniques were significantly hindered by time-consuming procedures, high equipment cost, or complex pre-separation. Thus, it is necessary to develop a cost-effective and high sensitive method to determine the level of VB₁₂.

Due to simple instruments and easy operation properties, fluorescence resonance energy transfer (FRET) techniques have received tremendous interests for detection of ions and small organic molecules,⁹⁻¹² that utilize energy transfer between two chromophores (one is as donor and another is an acceptor). Briefly, the donor is initially excited to high energy state and transfer energy to the acceptor via nonradiative dipole-dipole coupling.¹³ The FRET system should satisfy two conditions: (a) the emission spectrum of the donor and the absorption spectrum of the acceptor are appreciably overlapped to an extent; (b) the distance between donor and acceptor is in nanometer scale (1 to 10nm).

Carbon dots (CDs) have received tremendous attention due to their excellent tunable optical property, better photostability, easy fabrication, low cost and better biocompatibility.^{14, 15} In contrast to conventional fluorescent materials like organic dyes and rare earth quantum dots, the emission peak of CDs can be easily controlled in a big wavelength range with relatively small FWHM (full wavelength at half maximum), which make CDs appropriate to detect diverse bio organic molecules but only if the emission peak of CDs (donors) and the absorbance peak of bio-molecules (acceptors) are highly matched. Moreover, the surface structure of CDs can be easily engineered to demonstrate a strong bonding with specific detected acceptors, which allows for a short distance between CDs and acceptors. These excellent properties satisfy the requirements of FRET system and make CDs excellent potential donors in FRET optical systems with high selectivity and sensitivity.

In this paper, thermal reduction strategy was applied to obtain high luminescent CDs via heating at 300°C (as shown in scheme 1 (a)). Compared to other modification methods, the CDs would be less contaminated because no chemical reagents are used in this method.¹⁶⁻²³ Therefore, the thermal reduced CDs are suitable in bio and medical applications. The t-CDs based optical sensor was developed to determine the level of VB₁₂ (As shown in scheme 1 (b)). The limit of detection (LOD) was decreased from 0.4 μg/ml (LOD for CDs based optical sensor) to 0.1 μg/ml (100ppb), which was improved in comparison with CdTe QDs based optical sensor (LOD = 150ppb)²⁴ and close to conventional approaches like HPLC and chemiluminescence.



Scheme 1. (a) Thermal reduction process from CDs to t-CDs and (b) fluorescence resonance energy transfer process from t-CDs to Vitamin B₁₂

2. Experimental section

2.1 Materials

Citric acid, sodium hydrate, quinine sulfate and vitamin B₁₂ were purchased from Sigma-Aldrich. Dialysis bags (molecular weight cut off = 2000Da) were also ordered from Sigma-Aldrich. All reagents were used as received without any further purification.

2.2 Sample Preparation

CDs were prepared as described previously.²⁵ Briefly, 2 g CA were put into a 10 mL beaker and heated at 200°C on a hot plate. About 5 minutes later, the CA was liquated. Subsequently, the color of the liquid changed from colorless to pale yellow, and then orange after 30 minutes, implying the formation of CDs. The obtained orange liquid for preparing CDs was neutralized to pH 7.0 with 10 mg/ml NaOH solution.

The mixture was further dialyzed in a dialysis bag (retained molecular weight: 2000 Da) to obtain greenish yellow fluorescent CDs. The thermal reduction reactions were carried out in a thermo gravimetric analysis (TGA) instrument (Q50 TA). 3mg CDs were put onto a platinum pan and heated at 300 °C for 2 hours. After that, brightly blue luminescent t-CDs were obtained.

The CDs and t-CDs were dispersed in DI water and were both sonicated for 30 minutes in an ice bath, using a bath ultrasonicator (60W, frequency 40KHz, Model 2510, Branson) to achieve uniform and stable solutions (25µg/ml). VB₁₂ solution was prepared by dissolving the required amount of VB₁₂ powder in DI water. Then 200µl CDs solution or t-CDs solution was firstly added into a 5ml volumetric flask. After that, various specific amount of VB₁₂ solution was also added and finally the mixture was mixed with DI water to obtain 5ml solution. The concentration of CDs or t-CDs in mixture solution was kept at 10µg/ml and concentration of VB12 was varied from 0.04µg/ml to 12µg/ml.

2.3 Characterization

UV absorbance measurements were carried out on a JASCO V-550 UV-vis spectrophotometer, equipped with a Peltier temperature control accessory. Fluorescence spectra were measured on a FluoroMax-3 spectrofluorometer. All spectra were recorded in a 1.0 cm path length cell. FTIR characterization was

carried out on a Nicolet IS10 FTIR spectrometer by KBr pellet method. The samples were thoroughly ground with exhaustively dried KBr. XPS spectra were carried on X-ray photoelectron spectroscopy (XPS, PHI5000 Versa Probe). TEM images were recorded using a HITACHI 8100 transmission electron microscope operating at 75 kV. The zeta potential was characterized by a Malvern Zetasizer Nano ZS90 Dynamic Light Scattering. Quantum Yield (QY) Measurements were used to calculate the quantum yield of CDs and t-CDs. Quinine sulfate in 0.1M H₂SO₄ (QY = 0.54) was chosen as a standard. The quantum yields of CDs, t-CDs in water were calculated according to the formula: $\Phi = \Phi_s(I/I_s)(A/A_s)(n_s/n)$.²⁶ Where Φ is the quantum yield, I is the measured integrated emission intensity, n is the refractive index of the solvent (1.33 for water), and A is the optical density. The subscript "s" refers to the reference standard with known quantum yield.

3. Results and discussion

3.1 Structural Characterization

CDs which emit green luminescence were synthesized as previously reported,²⁵ and then they were thermally reduced at 300°C for 2 hours. The obtained thermal reduced CDs (t-CDs) showed an improvement in the photoluminescence intensity and the aqueous solution of t-CDs was stable for at least six months at room temperature. As shown in the Fig. 1 (a) and (b), the transmission electron microscope (TEM) images showed that both CDs and t-CDs were well dispersed and their size distribution were similar. It demonstrated that the thermal reduction made no major difference in the size of CDs. The dynamic light scattering results also presented the similar size distribution (4.8-9nm) and the similar average size (6nm) for CDs and t-CDs, as shown in Fig. 1 (d) and 1(e), which was consistent with the results of TEM. It indicated that the luminescent blue shift of t-CDs could result from the change of surface chemical structures and the decrease of surface defect after thermal reduction rather than size distribution. High-resolution TEM (HRTEM) image (Fig. 1(c)) reveals the crystallinity structure of the CDs, which is similar to that of many other reported CDs.²⁷⁻²⁹ Fourier transform infrared (FT-IR) spectroscopy was used to

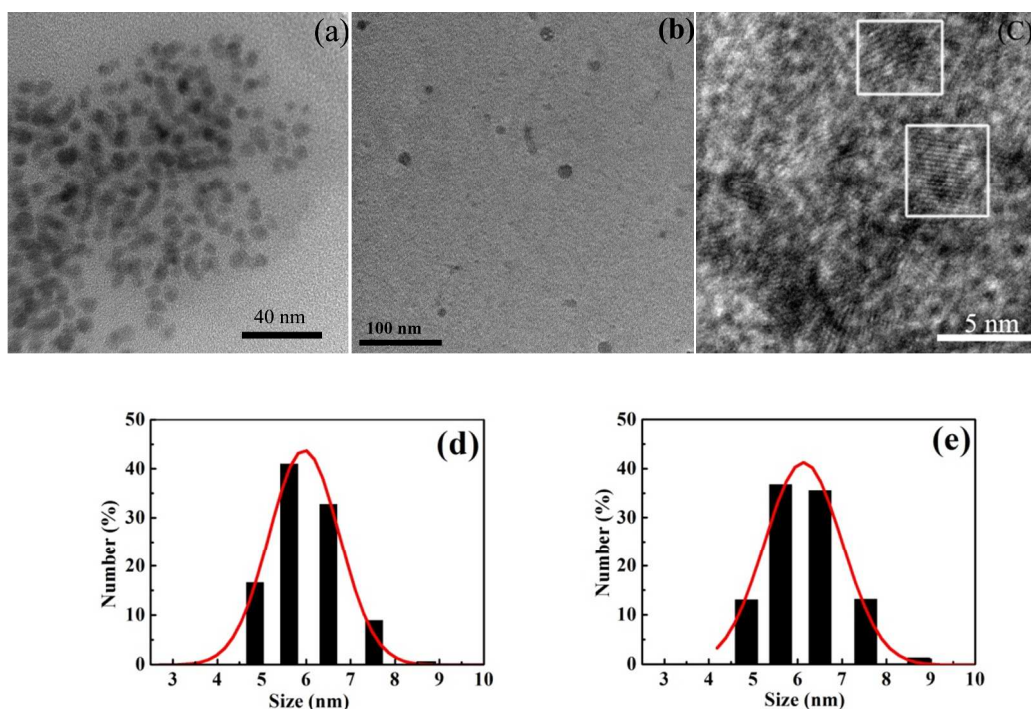


Figure 1. TEM images of (a) CDs and (b) t-CDs, High-resolution TEM (HRTEM) image of CDs (c) and size distribution of (d) CDs and (e) t-CDs via dynamic light scattering (DLS)

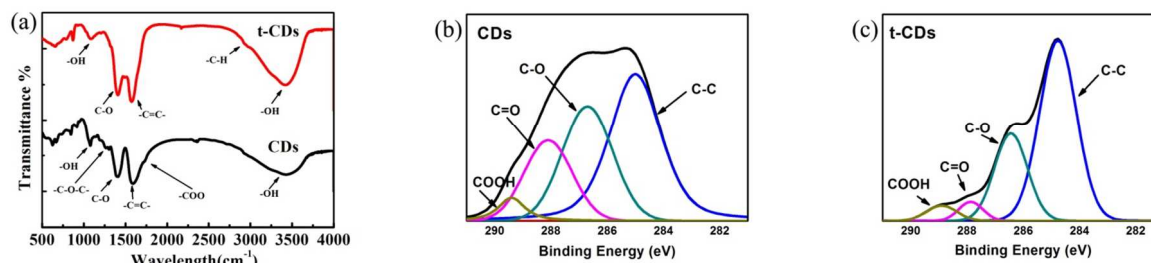


Figure 2. FT-IR spectra of t-CDs and CDs (a) and Deconvoluted XPS C1s core level spectra of CDs (b) and t-CDs (c)

further study the surface functional groups and chemical component of CDs and t-CDs. As shown in Fig. 2(a), the stretching vibrations of C-OH at 3430 cm^{-1} , $\text{C}=\text{C}$ at 1595 cm^{-1} and $\text{C}-\text{O}-\text{C}$ at 876 cm^{-1} were found for both CDs and t-CDs. However, the stretching vibration absorption bands of $-\text{COO}$ at 1715 cm^{-1} and $\text{C}-\text{O}-\text{C}$ at 1250 cm^{-1} were only observed for CDs. The vibration of C-OH, $\text{C}-\text{O}-\text{C}$ and $-\text{COO}$ for CDs indicated the existence of functional groups of hydroxyl, carboxyl and epoxy on the surface of CDs. After thermal reduction, the vibration absorption bands of $-\text{COO}$ at 1715 cm^{-1} and $\text{C}-\text{O}-\text{C}$ at 1250 cm^{-1} disappeared. Meanwhile, vibrations of $-\text{CH}$ at 2920 cm^{-1} were observed in t-CDs, demonstrating that the functional groups of $-\text{COO}$ are thermally reduced on the surface of t-CDs.³⁰ In addition, X-ray photoelectron spectroscopy (XPS) results (Fig. S1) indicate that the CDs and t-CDs are mainly composed of carbon and oxygen. The results demonstrate that the oxygen content is reduced after thermal reduction. The high-resolution spectrum of C1s exhibits four main peaks (Fig. 2b and c). The binding energy peak at 284.5 eV confirms the graphitic structure (sp^2 C-C) of the CDs and t-CDs. The peak at about 286.7 eV suggests the

presence of C-O, and the peak around 288.1 eV and 288.9 eV could be assigned to C=O and $-\text{COOH}$, respectively. After thermal reduction, the contents of C=O and $-\text{COOH}$ are decreased. The result is consistent with FTIR result.

The average zeta potential of CDs and t-CDs is $-21.36 \pm 1.38\text{ mV}$ and $-15.16 \pm 2.01\text{ mV}$ ($\text{pH}=7.0$), respectively. It indicates that thermal reduction decreased the surface charges of CDs due to the decrease of epoxy and carboxyl groups. These results are consistent with the FT-IR and XPS results.

3.2 Optical Characterization

The optical properties of CDs and t-CDs were studied using UV-vis absorption and photoluminescence spectroscopy. As shown in Fig. 3 (a), due to the $n-\pi^*$ transition, an obvious peak at 350 nm was observed in the UV-vis absorption spectra of CDs. In comparison, there was no obvious peak observed in UV-vis spectra of t-CDs, which was due to the decrease of carboxyl and epoxy groups during the thermal reduction process. As shown in Fig. 3 (b) and (c), the CDs showed the maximum excitation and emission wavelengths near 370 nm and 460 nm , whereas the

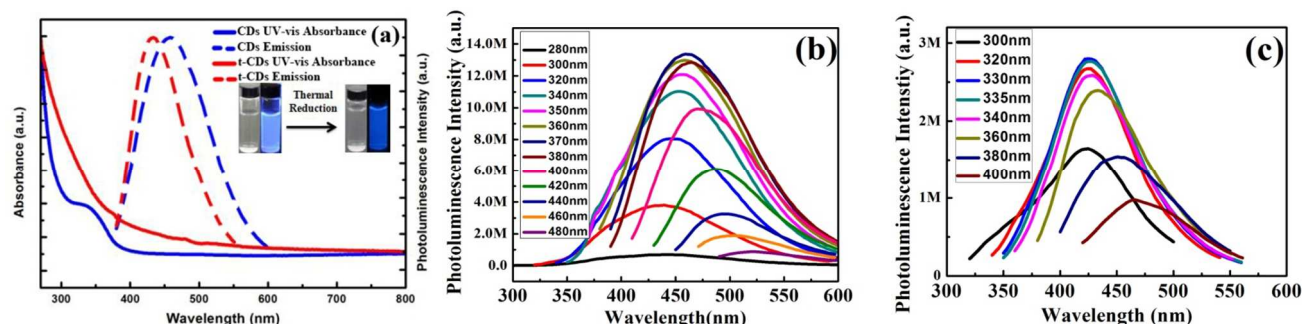


Figure 3. (a): UV-vis absorption and normalized photoluminescence spectra of CDs and t-CDs. Insert: photograph of the CDs (left) and t-CDs (right) aqueous solution under visible light and 365 nm UV light, respectively, (b): Emission spectra of the CDs with excitation of different wavelengths, (c): Emission spectra of the t-CDs with excitation of different wavelengths

Table 1. Quantum Yield of the as-synthesized CDs and t-CDs

Sample	Integrated emission Intensity (a.u.)	Absorbance at 340nm(a.u.)	Refractive index of solvent (n)	Quantum Yield (%)
Quinine sulfate	2504394589	0.0418	1.33	54%
CDs	211713269	0.0583	1.33	3.27%
t-CDs	988546174	0.0525	1.33	16.28%

maximum excitation and emission wavelengths of t-CDs were near 330nm and 420nm.

In contrast to CDs, a blue shift of the emission peak was observed in the photoluminescence spectra of t-CDs. This increase in the band gap was due to less carboxyl groups existing on the surface of the t-CDs. The CDs and t-CDs both exhibited excitation-dependent properties. The maximum emission wavelength of CDs was dependent on the excitation wavelength, shifting from 430-520nm when excited from 280-480nm. In comparison, the t-CDs had maximum emission wavelength ranged from 420-470nm, while the excitation wavelength ranged from 280-465nm. The broad and excitation-dependent emission of CDs and t-CDs presented the effects from different emission sites of each sp^2 clusters.^{31, 32} The imperfect absorption peak of CDs and broad absorption below 600nm of t-CDs both demonstrated those sp^2 clusters contained in CDs and t-CDs were not uniform in size.

The QY of the CDs and t-CDs at 340nm were 3.27% and 16.28%, respectively (selecting quinine sulfate as the standard), which indicated that thermal reduction could significantly improve the QY of CDs (As shown in table 1). Combining the results of FT-IR and XPS and the measurement of QY, the decrease of carboxyl group in t-CDs significantly enhanced the photoluminescence of CDs.³³ As shown in Fig. S2, the result shows good photostability of t-CDs in aqueous solution.

3.3 CDs and t-CDs for sensing VB_{12}

In order to detect VB_{12} in aqueous solution, the CDs and t-CDs based optical sensors were developed. As shown in Fig. 4a, VB_{12} has an obvious peak at 550nm in the range from 400 to 800nm, which is attributed to the $\pi-\pi^*$ transition. The photoluminescence

spectra of CDs and t-CDs at pH=7 were demonstrated in the Fig. 4 (b), where t-CDs presented 4 times higher luminescence intensity than that of CDs, which was consistent with the result of quantum yield of CDs (3.27%) and t-CDs (16.28%).

The integral overlap spectrum of the UV-vis absorbance spectrum of VB_{12} and the emission spectrum of CDs or t-CDs was showed in the Fig. 4 (c) and (d). These spectra exhibited an evident overlap between the luminescence spectrum of CDs or t-CDs and the absorption spectrum of VB_{12} . It indicated that the possibility of fluorescence resonance energy transfer process from CDs or t-CDs to VB_{12} . As shown in Fig. 4e, the fluorescence intensity vs the VB_{12} plot can be curve-fitted into $(I_0/I) = K_{SV}[VB_{12}] + 0.9769$, close to the Stern-Volmer equation with a correlation coefficient R^2 of 0.998 and K_{SV} is 38.337 mg/ml. Fig. S3 shows kinetic behavior of the fluorescence in t-CDs- VB_{12} system, which has long time stability.

The luminescence spectra of CDs or t-CDs at the presence of different concentrations of VB_{12} were presented in Fig. 5. The emission intensity of CDs or t-CDs decreased with enhancing concentration of VB_{12} , which indicated CDs- or t-CDs- VB_{12} system were efficient FRET system. Under the specified optimal reaction conditions, the linear calibration graphs were constructed for energy transfer efficiency of CDs or t-CDs for different concentrations of vitamin B_{12} samples. Each concentration was analyzed three times. The efficiency of fluorescence energy transfer process has been calculated from following equation

$$E = \frac{F_0 - F}{F_0} * 100\% \quad (1)$$

Cite this: DOI: 10.1039/c0xx00000x

www.rsc.org/xxxxxx

ARTICLE TYPE

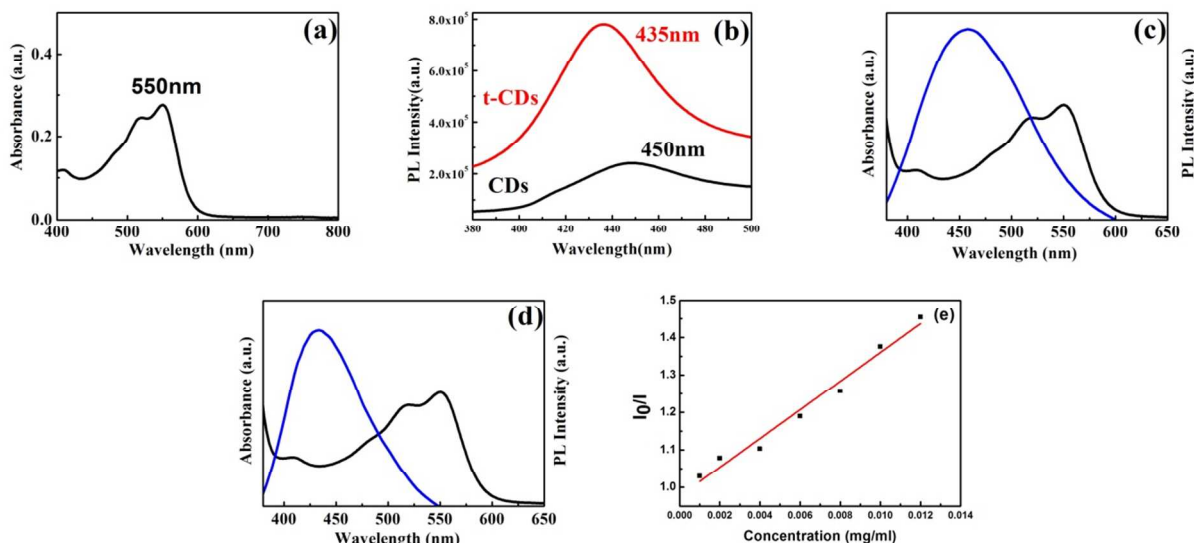


Figure 4. (a) UV-vis absorbance spectrum of vitamin B₁₂, (b) 0.01 mg/ml CDs and t-CDs PL intensity via 360 nm excitation, (c) the spectral overlap between the fluorescence of the CDs (360 nm excitation) and the absorbance spectrum of VB₁₂, (d) the spectral overlap between the fluorescence of the t-CDs (360 nm excitation) and the absorbance spectrum of VB₁₂, and (e) Stern–Volmer plot of CDs quenched by VB₁₂ aqueous solution

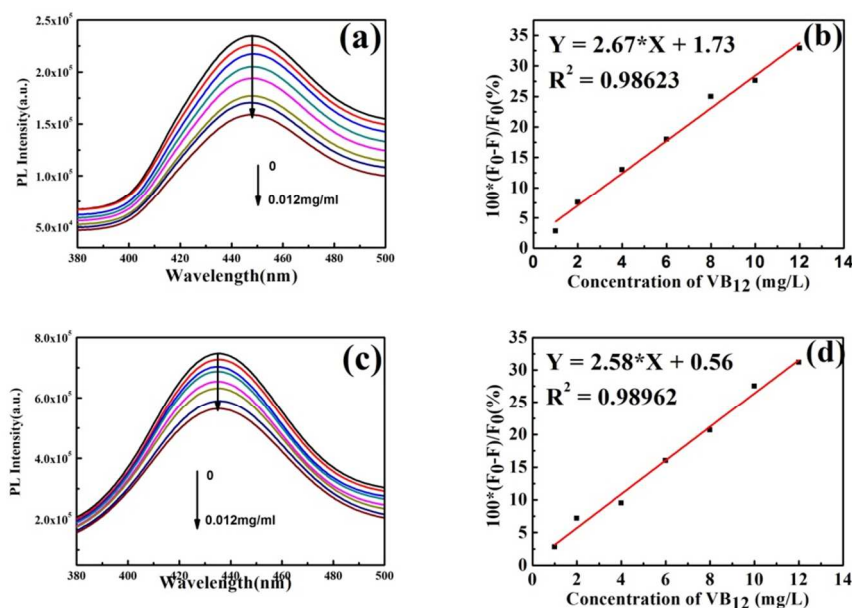


Figure 5. (a) Fluorescence quenching of CDs in the presence (black line) and absence (other colors) of concentration of vitamin B₁₂ from 1 to 12 µg/ml. (b) the plot of calibration graph for the efficiency of FRET process vs. concentration. (c) fluorescence quenching of t-CDs in the presence (black line) and absence (other colors) of concentration of vitamin B₁₂ from 1 to 12 µg/ml. (d) the plot of calibration graph for the efficiency of FRET process vs. concentration

where F is the donor fluorescence intensity in absence (F_0) and presence (F) of the acceptor. For 0.4 µg/ml addition of VB₁₂ to t-

CDs aqueous solution only 2% energy transfer occurs, whereas for 12 µg/ml addition the energy transfer is 31%, as shown in Fig. 5(c). It demonstrated that the efficiency of energy transfer increases with the gradual addition of VB₁₂. The same tendency is obtained from CDs and the energy transfer efficiency is 32% for the 12 µg/ml VB₁₂ addition, which is almost equal to that of t-CDs (31%), as shown in Fig. 5(a). It confirmed that CDs and t-CDs are both excellent donors in FRET process. It demonstrated that the reduced epoxy and carboxyl group did not diminish the efficiency of FRET process and the t-CDs still had strong affinity to VB₁₂. The graph of CDs and t-CDs in Fig. 5(b) and (d) were linear in the concentration range of 1-12 µg/ml with a correlation coefficient $R^2=0.98623$ and 0.98962 , respectively. The high correlation coefficient indicated that CDs or t-CDs based optical sensor had high detective accuracy.

According to IUPAC criterion,³¹ the limit of detection (LOD) is calculated as the concentration of VB₁₂ which produces an analytical signal that is three fold the standard deviation ($n=4$) of the blank signal. From this criterion, the standard deviation of the blank signal was an essential parameter to affect the LOD of optical sensor. For CDs based optical sensor, the standard deviation of photoluminescence intensity 1.87%, whereas the t-CDs based optical sensor was 0.36%, which was much smaller. It exhibited that as-synthesized t-CDs aqueous solution acquired more uniform and stable optical properties and higher photostability, due to decreased carboxyl group after thermal reduction. The carboxyl group had a significant impact on nonradiative recombination during surrounding change like pH.³⁴ Repeated experiment was performed to obtain LOD with various concentration of VB₁₂ in 10 µg/ml CDs or t-CDs aqueous solution. The LOD of CDs based optical sensor was 2 µg/ml, however the LOD of t-CDs based optical sensor was 0.1 µg/ml (as shown in Fig. S4 and S5). It demonstrated that the t-CDs based optical sensor obtained significantly higher sensitivity to detect VB₁₂ in contrast to CDs based optical sensor. As shown in Figure S6, the 100 µg/ml glycine, tyrosine and melamine is added into 25 µg/ml t-CDs solution, respectively. It is obvious to demonstrate that there is no evident change of PL intensity in presence of glycine, tyrosine and melamine, which shows the t-CDs-based sensor obtains good selectivity.

The LOD of t-CDs is 100 ppb, which is similar with that of CdTe quantum dots based FRET optical sensors (150 ppb [24]). However, the photoluminescence behaviors of t-CDs are tunable and their simple synthesis technology allows for mass production, which is significantly better than CdTe quantum dots based FRET optical sensor. In addition, as-synthesized t-CDs based FRET optical sensors possess more advantages like low cost, environmental friendly fabrication process. Moreover, the lower cytotoxicity and higher biocompatibility make it potential to detect VB₁₂ in vivo. The advantages discussed above demonstrate that t-CDs are superior in the FRET process to detect VB₁₂ in comparison with CdTe quantum dots.

4. Conclusion

In a summary, an environmentally benign method was firstly used to improve quantum yield of carbon dots via thermal reduction. Compared to the neat carbon dots, the thermal-reduced carbon dots demonstrated more uniform and stable optical

properties with significantly enhanced quantum yield. This is mainly due to reduced carboxyl group. The thermal-reduced carbon dots based fluorescence resonance energy transfer optical sensors were demonstrated to be very effective in the detection of VB₁₂ in aqueous solution with the concentration ranging from 1 to 12 µg/ml and their limit of detection (LOD) was as low as 0.1 µg/ml. The as-synthesized thermal-reduced carbon dots based optical probing technique demonstrates to be simple, cost-effective, sensitive and selective for detecting biologically significant VB₁₂. The present work may open a pathway for a facile and fast method to detect other small biomolecules through utilizing thermal-reduced carbon dots as the novel donor in FRET optical probes.

Acknowledgment

The authors would like to acknowledge the support from NSF grant #1228127. The authors thank Dr. Brandon Weeks for the UV-vis spectra characterization and Dr. Hope Weeks for their fluorescence spectra characterization.

Notes and references

^a Department of Mechanical Engineering, Texas Tech University, 2500 Broadway, P.O. Box 43061, Lubbock, TX 79409, United States
Corresponding Author: E-mail: Jenny.Qiu@ttu.edu

Reference

1. J. Zhang, Z. G. Tian, L. Liang, M. Subirade and L. Y. Chen, *Journal of Physical Chemistry B*, 2013, **117**, 14018-14028.
2. E. Alphonandery, S. Faure, O. Seksek, F. Guyot and I. Chebbi, *ACS Nano*, 2011, **5**, 6279-6296.
3. E. Alphonandery, C. Carvallo, N. Menguy and I. Chebbi, *Journal of Physical Chemistry C*, 2011, **115**, 11920-11924.
4. P. Tomcik, C. E. Banks, T. J. Davies and R. G. Compton, *Analytical Chemistry*, 2004, **76**, 161-165.
5. J. H. Chen and S. J. Jiang, *Journal of Agricultural and Food Chemistry*, 2008, **56**, 1210-1215.
6. Y. K. Zhou, H. Li, Y. Liu and G. Y. Liang, *Analytica Chimica Acta*, 1991, **243**, 127-130.
7. S. Wongyai, *Journal of Chromatography A*, 2000, **870**, 217-220.
8. K. Akatsuka and I. Atsuya, *Fresenius Zeitschrift Fur Analytische Chemie*, 1989, **335**, 200-204.
9. F. K. Du, Y. H. Ming, F. Zeng, C. M. Yu and S. Z. Wu, *Nanotechnology*, 2013, **24**.
10. C. M. Yu, X. Z. Li, F. Zeng, F. Y. Zheng and S. Z. Wu, *Chemical Communications*, 2013, **49**, 403-405.
11. L. S. Fan, Y. W. Hu, X. Wang, L. L. Zhang, F. H. Li, D. X. Han, Z. G. Li, Q. X. Zhang, Z. X. Wang and L. Niu, *Talanta*, 2012, **101**, 192-197.
12. S. H. Su, S. R. Wang and J. J. Qiu, *Science of Advanced Materials*, 2014, **6**, 203-208.
13. F. Aldeek, X. Ji and H. Mattoussi, *Journal of Physical Chemistry C*, 2013, **117**, 15429-15437.
14. X. M. Sun, Z. Liu, K. Welsher, J. T. Robinson, A. Goodwin, S. Zaric and H. J. Dai, *Nano Research*, 2008, **1**, 203-212.
15. Q. Qu, A. W. Zhu, X. L. Shao, G. Y. Shi and Y. Tian, *Chemical Communications*, 2012, **48**, 5473-5475.

16. J. L. Wang, Z. Zhou, X. Huang, L. W. Zhang, B. T. Hu, S. Moyo, J. Sun and Y. P. Qiu, *Journal of Adhesion Science and Technology*, 2013, **27**, 1278-1288.
17. H. J. Sun, L. Wu, N. Gao, J. S. Ren and X. G. Qu, *Acs Applied Materials & Interfaces*, 2013, **5**, 1174-1179.
18. Z. Zhou, X. C. Liu, B. T. Hu, J. L. Wang, D. W. Xin, Z. J. Wang and Y. P. Qiu, *Surface & Coatings Technology*, 2011, **205**, 4205-4210.
19. L. L. Li, J. Ji, R. Fei, C. Z. Wang, Q. Lu, J. R. Zhang, L. P. Jiang and J. J. Zhu, *Advanced Functional Materials*, 2012, **22**, 2971-2979.
20. J. H. Shen, Y. H. Zhu, C. Chen, X. L. Yang and C. Z. Li, *Chemical Communications*, 2011, **47**, 2580-2582.
21. J. H. Wei, J. J. Qiu, L. Li, L. Q. Ren, X. W. Zhang, J. Chaudhuri and S. R. Wang, *Nanotechnology*, 2012, **23**.
22. Z. Zhou, J. L. Wang, X. Huang, L. W. Zhang, S. Moyo, S. Y. Sun and Y. P. Qiu, *Applied Surface Science*, 2012, **258**, 4411-4416.
23. J. Wei, S. Jacob and J. Qiu, *Composites Science and Technology*, 2014, **92**, 126-133.
24. E. Vaishnavi and R. Renganathan, *Spectrochimica Acta Part a-Molecular and Biomolecular Spectroscopy*, 2013, **115**, 603-609.
25. Y. Q. Dong, J. W. Shao, C. Q. Chen, H. Li, R. X. Wang, Y. W. Chi, X. M. Lin and G. N. Chen, *Carbon*, 2012, **50**, 4738-4743.
26. Y. Wang, Q. Z. Lu, S. L. Wu, B. L. Karger and W. S. Hancock, *Analytical Chemistry*, 2011, **83**, 3133-3140.
27. S. N. Baker and G. A. Baker, *Angewandte Chemie-International Edition*, 2010, **49**, 6726-6744.
28. L. B. Tang, R. B. Ji, X. K. Cao, J. Y. Lin, H. X. Jiang, X. M. Li, K. S. Teng, C. M. Luk, S. J. Zeng, J. H. Hao and S. P. Lau, *Acs Nano*, 2012, **6**, 5102-5110.
29. S. J. Zhu, J. H. Zhang, S. J. Tang, C. Y. Qiao, L. Wang, H. Y. Wang, X. Liu, B. Li, Y. F. Li, W. L. Yu, X. F. Wang, H. C. Sun and B. Yang, *Advanced Functional Materials*, 2012, **22**, 4732-4740.
30. D. Y. Pan, L. Guo, J. C. Zhang, C. Xi, Q. Xue, H. Huang, J. H. Li, Z. W. Zhang, W. J. Yu, Z. W. Chen, Z. Li and M. H. Wu, *Journal of Materials Chemistry*, 2012, **22**, 3314-3318.
31. W. L. Wilson, P. F. Szajowski and L. E. Brus, *Science*, 1993, **262**, 1242-1244.
32. Y. P. Sun, B. Zhou, Y. Lin, W. Wang, K. A. S. Fernando, P. Pathak, M. J. Mezziani, B. A. Harruff, X. Wang, H. F. Wang, P. J. G. Luo, H. Yang, M. E. Kose, B. L. Chen, L. M. Veca and S. Y. Xie, *Journal of the American Chemical Society*, 2006, **128**, 7756-7757.
33. G. Eda, Y. Y. Lin, C. Mattevi, H. Yamaguchi, H. A. Chen, I. S. Chen, C. W. Chen and M. Chhowalla, *Advanced Materials*, 2010, **22**, 505-+.
34. A. Kundu, S. Nandi, R. K. Layek and A. K. Nandi, *Acs Applied Materials & Interfaces*, 2013, **5**, 7392-7399.

Table of Contents

Text: After thermal reduction, the quantum yield of thermal reduced-carbon dots demonstrated a 5-fold increment than original carbon dots.

GRAPHIC:

